International Journal Multidisciplinary
Homepage : https://journal.antispublisher.com/index.php/IJMI
Email : admin@antispublisher.com

e-ISSN : 3031-9870
IJMI, Vol. 3, No. 2, May 2026
Page 468-479

Numerical Investigation of Adatom-Adatom Interaction Effects on Surface Diffusion Dynamics in Two-Dimensional Materials

Rehab N. Hasnawi [1], Fatima H. Saeed [2]
[1,2] University of Basrah, Iraq

DOI : https://doi.org/10.61796/ijmi.v3i2.497

Sections Info

Article history:
Submitted: February 07, 2026
Final Revised: March 21, 2026
Accepted: April 15, 2026
Published: May 28, 2026

Keywords:
Adatom diffusion
Two dimensional materials
Adatom- adatom interactions
Nonlinear diffusion
Surface dynamics

ABSTRACT

Objective: *Adatom dynamics on the surfaces of two-dimensional (2D) materials is important for catalysis, nanoscale depositions, and electronic or optoelectronic applications. In this paper, we present a numerical treatment of the two-dimensional nonlinear diffusion equation dependent on the coverage function (θ) subject to Neumann boundary.* ***Method:*** *The adopted solution strategy is a hybrid of three techniques. The implicit Euler method is first used to discretize the time derivative leading to a second - order nonlinear partial variables. Secondly, the two dimensional is completely discretized by using second-order central difference approximations in time-finite different method giving non-linear algebraic equation. At last, an approximate solution are obtained iteratively by using Newton method.* ***Results:*** *We show that adatom- adatom interactions are essential for governing surface diffusion behavior on two-dimensional, thus providing guidance for nanomaterial design and potentially nanoelectronic device engineering.* ***Novelty:*** *The adopted solution strategy is a hybrid of three techniques.*

INTRODUCTION

A few tricks from the world of materials science, which has seen explosive growth since the work on two-dimensional (2D) materials was first discovered and in vogue in recent years. These materials are characterized by remarkable physical and chemical properties resulting from one- dimensional quantum confinement [1]. Graphene is one of its main representatives. The performance usually depends on their intrinsic impurities and adsorbed adatoms [2], [3], [4], [5]. Surface diffusion, as one of the original important phenomena like crystal defects and grain boundaries that control the behavior of adatoms [6], [7], is a principal process contributing to the stabilization of adatoms upon surface [2], [8]. This diffusion process is determined by the nature of the adsorbed species, Surface coverage density, presence defects in depth of lattice [5], [6], [7] and lateral interaction between adatom [2], [9]. Due to the complexity of this phenomenon, it necessitates the use of advanced numerical techniques for its simulation. The literature contains many studies that advanced this field of investigation: from pioneering work by Bernard and Buts in the 1980s about sulfur and oxygen diffusion on metal surfaces [10], [11], to investigations exploring lateral interactions effects with laser diffraction using Asscher's part modeling[9], to recent works such as those of Gaididei,Yan, Kazem which primarily dealt with atomic interaction modeling and their importance for adatom diffusion modeling for nanoelectronics applications [12], [13]. The present work addressed the temperature effects on lithium atom diffusion kinetics in two-dimensional

(2D) materials, as well as the variations of these parameters due to different impact of Surface coverage producing mediated repulsive interactions among adsorbed adatoms affecting the barrier heights.

RESEARCH METHOD

Two-dimensional materials

Two-dimensional materials

Two-dimensional (2D) materials are materials that consist of a single layer of atoms [20]. These materials are characterized by unique and interesting properties, making , among the notable examples [14]them promising for a wide variety of applications were shown in Figure 1.

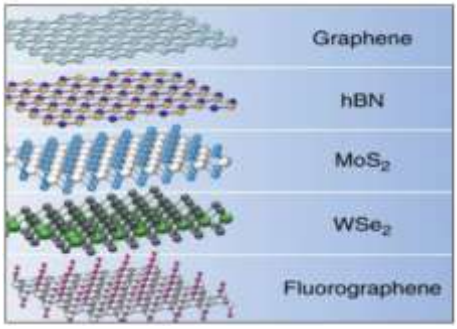

Figure 1. Represents some examples of two-dimensional (2D) materials [15].

Adsorbate surface diffusion is an area where the importance of two-dimensional materials, due to their unique physicochemical properties, is particularly important. More precisely, the effects of quantum confinement in out of plane dimension relying on adsorbates make a larger contribution to diffusion kinetics and accessibilities towards active sites and thus result in improvements across various areas including device performance efficiency.

Surface diffusion potential barrier

Adatom diffusion constitutes the fundamental process governing the growth dynamics of ultrathin films on 2D materials such as graphene. From a surface physics standpoint, 2D materials can be effectively modeled as conventional metallic surface with well-defined physical parameters. The surface lattice plays a critical role in determining the preferred adsorption sites for atoms or molecules, adsorbates do not attach randomly but preferentially occupy sites exhibiting the highest binding energy, Figure 2, such as:

Top site
Bridge site
Hollow site, which is commonly observed on the surfaces of 2D materials [16].

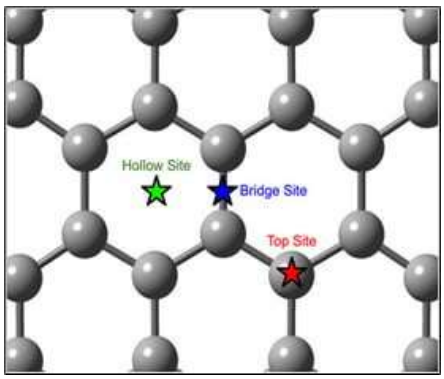

.[12] Figure 2. Possible sites for atom adhesion

The random walk model is the theoretical framework for surface diffusion most widely accepted. Surface diffusion, therefore, is not one that has a single activation energy barrier, but a spectrum of transition pathways and their hopping rates governing the overall nanoscale diffusion dynamics on the Surface [14].

RESULTS AND DISCUSSION

Mathematical Model of Surface Diffusion

The diffusion dynamics of adsorbed atoms (adatoms) on the surface of 2D materials, including graphene [17], hexagonal boron nitride (h-BN) [14], and molybdenum disulfide (MOS2) [14]. It is based on the fact that, via lateral interaction between atoms, the diffusion coefficient varies with respect to surface diffusion coverage [10], [13].

The (2D) diffusion equation is formulated as follows:

$$\frac{\partial\theta(x,y,t)}{\partial t} = \bar{\nabla}.\left(D\left(\theta(x,y,t)\right)\bar{\nabla}\,\theta(x,y,t)\right) \qquad (1)$$

Where $\theta(x,y,t)$ represents the surface coverage density (number of atoms per unit area), and $D(\theta)$ is the coverage-dependent diffusion coefficient. Expanding the derivatives in cartesian coordinates yields the following nonlinear from:

$$\frac{\partial\theta(x,y,t)}{\partial t} = \frac{\partial D_{(\theta)}}{\partial\theta}\left[\frac{\partial^2\theta}{\partial x^2} + \frac{\partial^2\theta}{\partial y^2}\right] + D(\theta)\left[\left(\frac{\partial\theta}{\partial x}\right)^2 + \left(\frac{\partial\theta}{\partial y}\right)^2\right] \qquad (2)$$

Equation (2) becomes a linear (equivalent) partial diffusion equation when $\frac{\partial D(\theta)}{\partial\theta} = 0$, that is, when D is independent of θ. Equation (2) is a nonlinear partial differential equation with time-dependent boundary conditions where $\frac{\partial D(\theta)}{\partial\theta} \neq 0$.

$$\theta(a,t) = \alpha(t), \theta(b,t) = \beta(t) \qquad t > 0 \qquad (3)$$
$$\theta(c,t) = \alpha(t), \theta(d,t) = \beta(t) \qquad t > 0$$

where the coverage at the surszsaface boundaries depends only on time, while the initial conditions are as follows:

$$x = 0, \frac{\partial\theta}{\partial x} = \theta, \qquad y = 0, \frac{\partial\theta}{\partial y} = \theta \qquad (4)$$

$$x = L, \frac{\partial\theta}{\partial x} = -\theta \qquad , \quad y = L, \frac{\partial\theta}{\partial y} = -\theta \qquad (5)$$

Temporal Discretization Using Implicit Euler Method

First, we use a time step τ to discretize Equation (2) in time. The uniform division axis t>0 into grid points is based on [12].

$$\tau_n = n\tau\,, \qquad n = 0, 1, 2 \tag{6}$$

$$\frac{\theta_n - \theta_{n-1}}{\Delta t} = \partial_\theta D(\theta_n)\left[\left(\frac{\partial \theta_n}{\partial x}\right) + \left(\frac{\partial \theta_n}{\partial y}\right)\right] + D(\theta_n)\left[\frac{\partial^2 \theta_n}{\partial x^2} + \frac{\partial^2 \theta_n}{\partial y^2}\right] \tag{7}$$

Where $\theta_n = \theta(x, y)$, $\theta_{n_1} = \theta_{n_1}(x, y)$ are approximations to $\theta(x, y, \tau_{n-1})$ and $\theta(x, y, \tau_n)$, respectively. Equation (12) can be written as:

$$\frac{\partial^2 \theta_n}{\partial x^2} + \frac{\partial^2 \theta_n}{\partial y^2} = f(\theta_n\,, w_n\,, v_n\,, \theta_{n-1}\,) \tag{8}$$

Where $v_n = \frac{\partial \theta_n}{\partial x}$, $w_n = \frac{\partial \theta_n}{\partial y}$ are the spatial gradients of the surface coverage θ_n and f denotes a nonlinear function; consequently, the system can be expressed as:

$$f(\theta_n\,, w_n\,, v_n\,, \theta_{n-1}\,) = \frac{\emptyset(\,\theta_n\,, w_n\,, v_n\,, \theta_{n-1}\,)}{D(\theta_n)} \tag{9}$$

$$\emptyset(\,\theta_n\,, w_n\,, v_n\,, \theta_{n-1}\,) = \frac{\theta_n - \theta_{n-1}}{\Delta t} - \partial\theta\, D(\theta_n)[v^2 + w^2] \tag{10}$$

Equation (6) and boundary conditions

$$\theta_n(x, c) = \alpha(t_n)\,, \quad n(x) \tag{11}$$

$$\theta_n(x, d) = \beta(t_n)\,, \quad n(x) \tag{12}$$

$$\theta_n(a, y) = \alpha(t_n)\,, \quad n(y) \tag{13}$$

$$\theta_n(b, y) = \beta(t_n)\,, \quad n(y) \tag{14}$$

Where $\alpha_{v(\,.\,,\,t_n)} = \alpha_v$, v = 1, 2, 3, 4. A nonlinear boundary value problem (BVP) for the unknown, where $\alpha_{v(\,.\,,\,t_n)} = \alpha_v$, v = 1, 2, 3, 4. The nonlinear boundary value problem (BVP) for unknown function in the figures a,c shows that. Once (the solution function) is known, the problem becomes an instance of numerical analysis suitable for nonlinear problems. Following this, we perform a similar procedure for the initial condition as given above together with the boundary conditions to [10] access the coverage distribution of these adatoms in time, where n = 1, 2, 3. We will use the Finite Difference Method (FDM) and Newton method for this solution [18].

Newton's methodIts general name is the Newton-Raphson method, which has the advantages of stability and rapid convergence, It comes in quadratically converging. To apply Newton's method, we will need to find partial derivatives of the function with respect to. For the purpose of exposition, we have made some notations and used symbols.

$\emptyset_n = \emptyset(\,\theta_n\,, w_n\,, v_n\,, \theta_{n-1})$ $\qquad f_n = f(\theta_n\,, w_n\,, v_n\,, \theta_{n-1}\,)$

To denote the partial derivatives of f_n, we use:

$$p_n = p(\,\theta_n\,, w_n\,, v_n\,, \theta_{n-1}\,) \tag{15}$$

$$Q_n = q(\,\theta_n\,, w_n\,, v_n) \tag{16}$$

$$r_n = r(\,\theta_n\,, w_n\,, v_n\,) \tag{17}$$

$$q_n = \frac{\partial \emptyset_n}{\partial \theta_n} = \frac{1}{D(\theta_n)}\left[\frac{\partial f_n}{\partial \theta_n} - \emptyset\,\frac{\partial D(\theta_n)}{\partial \theta_n}\right] \tag{18}$$

$$p_n = \frac{\partial \emptyset_n}{\partial v_n} = \frac{1}{D(\theta_n)} \frac{\partial f_n}{\partial v_n} \quad (19)$$

$$r_n = \frac{\partial \emptyset_n}{\partial w_n} = \frac{1}{D(\theta_n)} \frac{\partial f_n}{\partial w_n} \quad (20)$$

Where:

$$\frac{\partial f_n}{\partial \theta_n} = \frac{1}{\Delta t} - \frac{\partial^2 D(\theta_n)}{\partial \theta^2} [v_n^2 + w_n^2] \quad (21)$$

$$\frac{\partial f_n}{\partial v_n} = -2 \frac{\partial D(\theta_n)}{\partial \theta} . v_n \quad (22)$$

$$\frac{\partial f_n}{\partial w_n} = -2 \frac{\partial D(\theta_n)}{\partial \theta} . w_n \quad (23)$$

These equations will be useful when calculating the elements of the inverse matrix for Newton's finite difference method.

Spatial Discretization Using Finite Difference Method (FDM)

In each of grid's spatial directions, we split the interval [c, d] = [a, b] in to N equal subintervals [14]. Where the step size is $h = \frac{b-a}{N-1}$.

$$x_i = a + (i-1)h \quad , i = 1,2,3 \ldots \ldots \quad (24)$$

$$x_j = a + (j-1)h \quad , j = 1,2,3 \ldots \ldots \quad (25)$$

Equation (8) is discretized using the Finite Difference Method with central difference approximation on the structured grid described by (24,25). With the border condition $i = 2, \ldots \ldots N-1$; $j = 2, \ldots \ldots N-1$. Using the central difference approximation for the second derivative using the finite difference method (FDM), which requires the following formula:

$$\frac{\theta_{n,j-1} , j - 2\theta_{n,i,j} + \theta_{n,i+1,j}}{h^2} + \frac{\theta_{n,i,j-1} - 2\theta_{n,i,j} + \theta_{n,i,j+1}}{h^2} = \emptyset(\theta_{n,i,j}, v_{n,i,j}, w_{n,i,j}, \theta_{n-1,i,j}) \quad (26)$$

where (w_n, I, j, v_n, I, j) are expressed as follows:

$$v_n, i, j = \frac{\theta_{n,i+1} , j - \theta_{n,i-1,j}}{2h^2} \quad (27)$$

$$w_n, i, j = \frac{\theta_{n,i,j+1} - \theta_{n,i,j-1}}{2h^2} \quad (28)$$

Solve the nonlinear system using Newton's method

Along with the boundary conditions, equation (26) creates a nonlinear system of N algebraic equations in unknown functions G_n, I, j. Newton's iteration technique will be used to solve this nonlinear system, and a vector G_n will be inserted, which writes as follows:

$$G_n = [G_n, 1,1, G_n, 1,2, \ldots \ldots, G_n, 1, N, \ldots \ldots, G_n, N, 1, G_n, N, 2, \ldots \ldots G_n] \quad (29)$$

with G_n, I, j corresponding to the boundary grid points defined as:

$$G_{n,i,j} = \theta_{n,i,j} - \alpha_{1,n,i,j} \quad j = 1, 1 \le i \le N \quad (30)$$

$$G_{n,i,j} = \theta_{n,i,j} - \beta_{1,n,i,j} \quad j = M, 1 \le i \le N \quad (31)$$

$$G_{n,i,j} = \theta_{n,i,j} - \alpha_{2,n,i,j} \qquad i = 1, 1 \le j \le N \tag{32}$$

$$G_{n,i,j} = \theta_{n,i,j} - \beta_{2,n,i,j} \qquad i = N, 1 \le j \le N \tag{33}$$

In light of this, the matrix $G_{n,I,j}$ is as follows:

$$G_{n,i,j} = \theta_{n,i+1,j} + \theta_{n,i+1,j} - 4\theta_{n,i,j} + \theta_{n,i,j-1} + \theta_{n,i,j+1} - h^2 \emptyset_{n,i,j} = 0 \tag{34}$$

For a single equation, the nonlinear algebraic system as in (21), together with the boundary conditions in (3,4,) and (5), is:

$$G_{n,i,j} = 0 \tag{35}$$

where:

$$\theta_n^{(k+1)} = \theta_n^{(k)} - \left(\left(L_n^{(k)}\right)^{-1}\right) G_n\left(\theta_n^k\right) \quad , k = 1,2,3 \ldots \ldots \tag{36}$$

Here, $L_n^{(k)}$ is N, N the times Jacobian matrix of G_n with regard to θ_n evaluated at θ_n^k the Jacobian matrix G_n is provided by:

$$L_{i,j,r,s} = \frac{\partial G_{n,i,j}}{\partial \theta_{n,r,s}} \tag{37}$$

Diffusion graphene adatom

Take the example from Ref [12]. It investigates the role of lithium adatoms to be adsorbed on cc and how the coverage by an adsorbate changes the diffusion barrier. The results show that after adsorption, the lithium atom loses part of its electronic charge and becomes partially positively charged. The ionic mechanism comes from the electronic charge transfer from lithium adatom to graphene substrate during its adsorption, which is essential for applications in lithium storage in carbon-based materials and understanding of lithium-ion battery. The surface diffusion coefficient, which is a coverage-dependent property, is fundamental to the modeling of thin-film growth in nano-scale devices. Here, we exploit the exact theoretical results given in the previous reference to find a mathematical form of the coverage- dependent surface diffusion coefficient of lithium adatoms on graphene. We collected diffusion barrier data, at different coverage values through Density Functional Theory (DFT) calculations, fitted them with an appropriate mathematical model (as shown in Figure 3), and combined this with a physical model for the most stable hollow (Hol) site of adsorption on CxNys respectively [12] to create chemical perception.

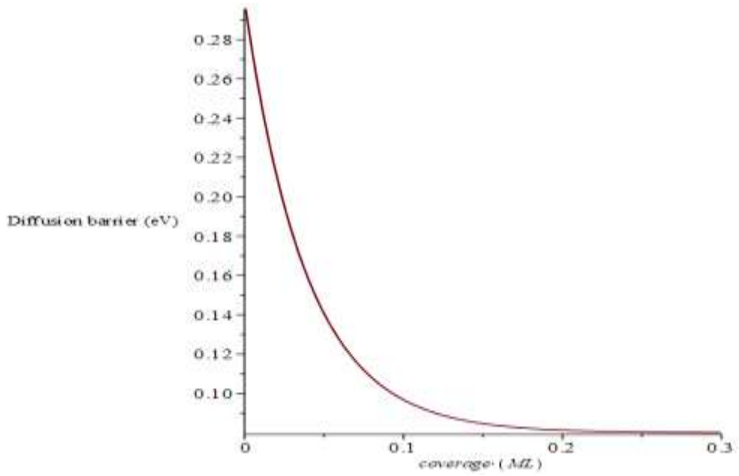

Figure 3. Show the product efficiency.

In Figure 3, shows an exponential decay of barrier energy with increasing surface coverage indicative of repulsive adsorbate interactions between neighboring adatoms that destabilize individual adatom adsorption at high coverages. This type of non-repulsive interaction effectively reduces the energy barrier for hopping, thus allowing adatom diffusion across the surface. The Arrhenius relation describes the surface diffusion coefficient [14].

$$D(\theta) = D_0 \exp\left(-\frac{E_{diff}}{K_B T}\right)$$

Where:

D_0:pre-exponential factor (constant)

E_{diff} : diffusion barrier energy, which is a function of surface

θ : coverage

K_B : Boltzmann constant

T : absolute temperature (held constant at 300K, as in Ref [14])

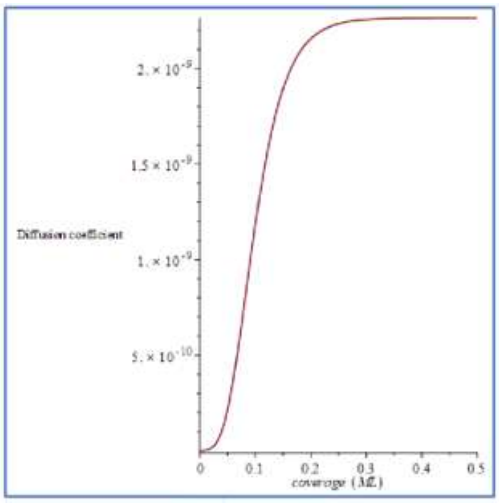

Figure 4: illustrates the coverage- dependent surface diffusion coefficient for adsorbed lithium ions on graphene at three distinct temperatures.

From looking at Figure 4, it clearly shows that surface diffusion coefficient increases with increases coverage due to the strong repulsive interaction of lithium adatom. These dreadfully hateful interactions decrease the ecstatic diffusion barrier and encourage adatom mobility. The proposed model can by comparison with previous experimental and theoretical results [13].

i. This model could be incorporated in numerical simulations of diffusion equation, such as those given by Fick's second law [14], [19], where the diffusion coefficient D is depending on temperature and features of substrates. Nevertheless, surface coverage has a strong impact on the surface diffusion coefficient by means of lateral adsorbate– adsorbate interaction (attraction or repulsion) [11a]. From Figs 1 & 2, it is clear that:
ii. At low coverage, repulsive interaction is weak, the diffusion barrier E_{diff} is high, and consequently $D(\theta)$ is low.
iii. At high coverage, repulsive interaction becomes pronounced, E_{diff} reduced, and $D(\theta)$ increases by several orders of magnitude.

This behavior suggests that repulsive lateral interactions speed up surface diffusion (at a fixed growth dynamics of ultrathin/multilayer films on graphene. The analytical expression derived for was then applied to calculate the temporal evolution of surface coverage, to study the time-dependent diffusion dynamics of adsorbed lithium atoms on a square graphene sheet with side length (hypothetical model system). We took a Gaussian profile to describe the initial distribution of adatoms at time The evolution of the coverage distribution is shown in Figure 5.

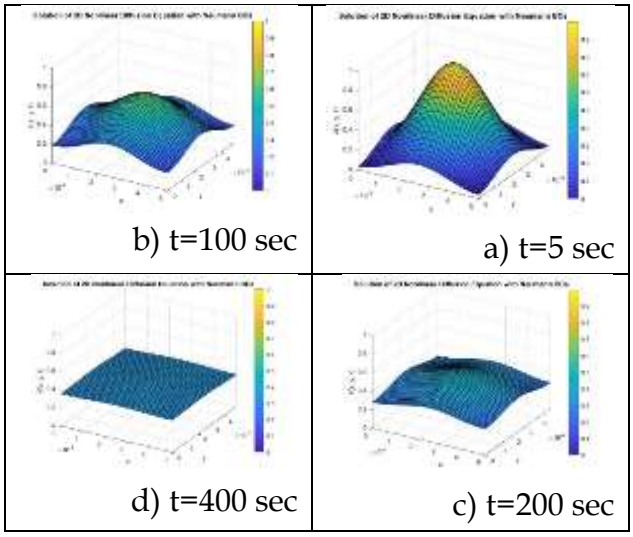

Figure 5: illustrates the temporal evolution of adsorbed lithium atom diffusion graphene at a temperature of 300K, under conditions where repulsive interactions between adsorbed adatoms are explicitly accounted for.

As observed from the figure, the diffusion process attains equilibrium after approximately 400s, corresponding to a final surface coverage of 3.8 monolayers (ML) at 300K.

Effect of Temperature on Diffusion

This behavior suggests that repulsive lateral interactions speed up surface diffusion (at a fixed growth dynamics of ultrathin/multilayer films on graphene. The analytical expression derived for was then applied to calculate the temporal evolution of surface coverage, to study the time-dependent diffusion dynamics of adsorbed lithium atoms on a square graphene sheet with side length (hypothetical model system). We took a Gaussian profile to describe the initial distribution of adatoms at time The evolution of the coverage distribution is shown below.

$$D(T) = D_o e^{-\frac{E_A}{K_B T}}$$

Where E_A represents the effective activation energy for diffusion, which as previously discussed, is approximately equivalent to the diffusion barrier height E_{diff}. The Figure 6, below illustrates $D(T)$ for three distinct temperatures.

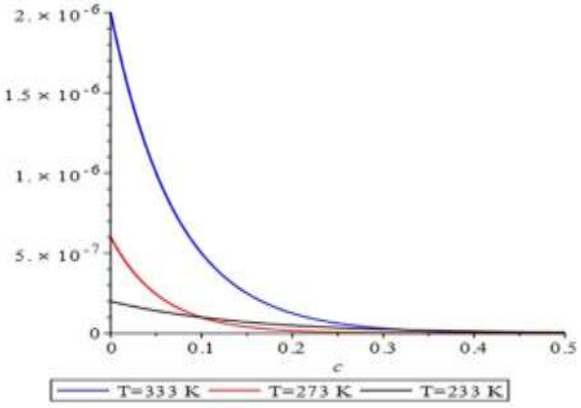

Figure 6: illustrates the coverage- dependent surface diffusion coefficient for adsorbed lithium ions on graphene at three distinct temperatures.

As observed from the figure above, the diffusion coefficient increases with in increases temperature across all coverage degrees. This behavior is physically expected, as elevated temperatures provide adsorbed atoms with greater thermal energy to overcome energy barriers during the diffusion process.

Furthermore, the effect of surface coverage whether low or high (depending on the concentration of adsorbed lithium atoms) significantly influences the activation energy, which is closely related to the diffusion barrier. In the case of low coverage, repulsive interactions between adsorbed adatoms are relatively weak. However, at high coverage, the activation energy increases, indicating that repulsive interactions between adatoms impede the diffusion process, thereby reducing the enhancing effect of elevated temperature on diffusion compared to the low-coverage regime. This behavior is clearly illustrated by the temporal evolution of lithium atom diffusion on the graphene surface at three distinct temperatures: as temperature increases, the diffusion rate correspondingly accelerates, as detailed in Figure 7.

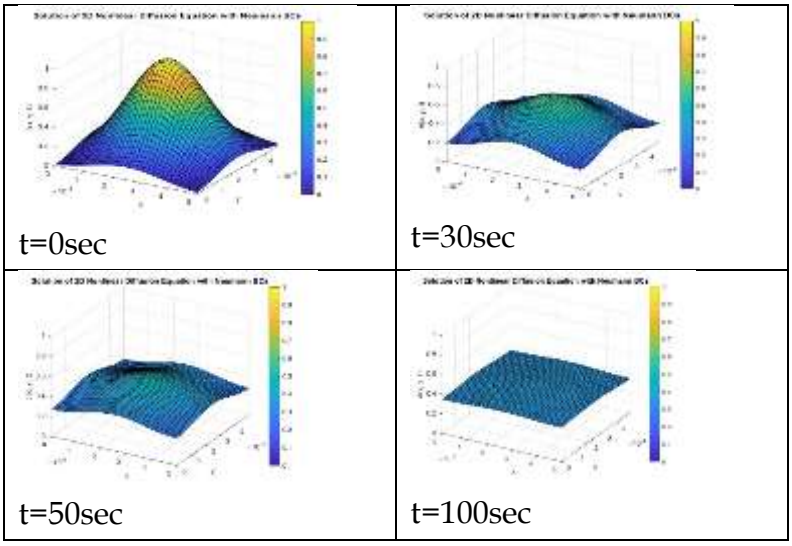

Figure 7. Illustrates the spatial distribution of lithium atoms adsorbed on the graphene surface at a temperature of T=233K and at successive time intervals (t=0,30,50,100s).

The remaining figures exhibit analogous temporal evolution behavior at the other investigated temperature (T=273, 233). The table below summarizes the variation in diffusion kinetics as a function of temperature.

Temperatures (K)	**Heat Energy K_BT (ev)**	**Time to Equilibrium t(s)**	**Notes**
233	0.02008	100	Slow Diffusion
273	0.02352	70	Faster Equilibrium, More Distribution
333	0.02874	50	Rapid diffusion

CONCLUSION

Fundamental Finding: The outcomes showed that the Hollow (Hol) site currently is the least energetically stable adsorption configuration, which is followed by the Bridge (Bri) site then finally the On-Top site (OT) frontier; this stability hierarchy does not depend on surface coverage. In addition, repulsive interactions between adsorbed lithium adatoms were revealed as the main mechanism causing both the decrease in adsorption energy and diffusion barriers with increasing surface coverage. The spatiotemporal evolution of the surface coverage distribution simulated showed that minimum energy path for lithium atom diffusion is from a Hollow (Hol) site to an adjacent Hollow site through Bridge (Bri) site, which is in accordance with those obtained

by Potential Energy Surface(PES) calculations. The results showed that the dynamic equilibrium of the diffusion happened after around 400 seconds at 300k and surface coverage completed with value of 3.8ML. The simulations showed a substantial increase in diffusion rate due to higher temperatures, which significantly reduced the time taken to achieve equilibrium, but non-linearly with the applied temperature. **Implication:** This study provides strong evidence for the important role of lateral adatom-adatom interactions in determining surface diffusion phenomena on 2D materials. Such discoveries provide exciting new pathways for applications ranging from nanomaterial design, and catalytic surface engineering to nano-electronic device working regimes and lithium-ion battery electrode optimization through controlling atomic-scale facet shape evolution during surface diffusion processes. **Limitation:** The study used theoretical data from Density Functional Theory (DFT) calculations, which created the quantitative relationship between diffusion barrier energy and surface coverage. Three principal adsorption positions, namely: On-Top position (OT), Bridge position (Bri) and Hollow position (Hol), were study in order to evaluate the lithium atoms adsorption on graphene. **Future Research:** Additionally, the Arrhenius equation was applied to determine the relationship between diffusion kinetics and temperature. Diffusion kinetics are studied by the Arrhenius equation based on the simulation.

REFERENCES

[1] C. L. Tan *et al.*, "Recent advances in ultrathin two-dimensional nanomaterials," *Chem. Rev.*, vol. 117, no. 9, pp. 6225–6331, 2017, doi: 10.1021/acs.chemrev.6b00558.

[2] B. G. Koehler and S. M. George, "Coverage dependence of the surface diffusion coefficient for hydrogen on Ru(001)," *Surf. Sci.*, vol. 191, no. 1–2, pp. 117–132, 1987, doi: 10.1016/0039-6028(87)90339-5.

[3] A. A. Peyghan, M. Noei, and M. B. Tabar, "A large gap opening of graphene induced by the adsorption of Co on the Al-doped site," *J. Mol. Model.*, vol. 19, no. 8, pp. 3007–3014, 2013, doi: 10.1007/s00894-013-1848-2.

[4] M. Sun, M. Re Fiorentin, U. Schwingenschlögl, and M. Palummo, "Excitons and light-emission in semiconducting $MoSi_2X_4$ two-dimensional materials," *NPJ 2D Mater. Appl.*, vol. 6, no. 1, p. 81, 2022, doi: 10.1038/s41699-022-00354-4.

[5] L. Si *et al.*, "A first-principles study of lithium adsorption and diffusion on graphene and defective-graphene as anodes of Li-ion batteries," *Coatings*, vol. 16, no. 1, p. 52, 2026, doi: 10.3390/coatings16010052.

[6] J. Cottom, Q. Cai, and E. Olsson, "Vacancy enhanced Li, Na, and K clustering on graphene," *Sustain. Energy Fuels*, vol. 9, no. 10, pp. 2813–2826, 2025, doi: 10.1039/D5SE00130G.

[7] C. Yang, R. Amirbeigiarab, S. Buttenschön, E. Pehlke, and O. M. Magnussen, "Non-monotonic variation of potential-dependent surface diffusion at electrochemical interfaces in the presence of coadsorbates," *Angew. Chem. Int. Ed.*, vol. 64, no. 10, p. e202419390, 2025, doi: 10.1002/anie.202419390.

[8] K. R. Khalaf and F. H. Saeed, "A numerical solution for the coverage-dependent surface diffusion equation in ultra-thin film," *IOSR Journal of Applied Physics*, vol. 14, no. 1, pp. 58–68, 2022, doi: 10.9790/4708-1401015766.

[9] Z. Ji, F. F. Contreras-Torres, A. F. Jalbout, and A. Ramírez-Treviño, "Surface diffusion and coverage effect of Li atom on graphene as studied by several density functional theory methods," *Appl. Surf. Sci.*, vol. 285, pp. 846–852, 2013, doi: 10.1016/j.apsusc.2013.08.140.

[10] R. Butz and H. Wagner, "Diffusion of oxygen on tungsten (110)," *Surf. Sci.*, vol. 63, no. 3, pp. 448–459, 1977, doi: 10.1016/0039-6028(77)90207-0.

[11] W. J. Bernard, C. M. Ablow, and H. Wise, "Surface diffusion of chemisorbed sulfur on nickel (111)," *Applications of Surface Science*, vol. 18, no. 4, pp. 429–436, 1984, doi: 10.1016/0378-5963(84)90004-3.

[12] Y. B. Gaididei, V. M. Loktev, A. G. Naumovets, and A. G. Zagorodny, "Adatom interaction effects in surface diffusion," 2012.

[13] K. Zhong, Y. Yang, G. Xu, J.-M. Zhang, and Z. Huang, "An ab initio and kinetic Monte Carlo simulation study of lithium ion diffusion on graphene," *Materials*, vol. 10, no. 7, p. 761, 2017, doi: 10.3390/ma10070761.

[14] V. G. Palomar, "Metal film growth on weakly-interacting substrates: Multiscale modeling," Linköping University, 2020. doi: 10.3384/diss.diva-171435.

[15] P. A. Khomyakov, G. Giovannetti, P. C. Rusu, G. V Brocks, J. den Brink, and P. J. Kelly, "First-principles study of the interaction and charge transfer between graphene and metals," *Phys. Rev. B*, vol. 79, no. 19, p. 195425, 2009.

[16] Y. G. Zhou, X. T. Zu, F. Gao, H. F. Lv, and H. Y. Xiao, "Adsorption-induced magnetic properties and metallic behavior of graphene," *Appl. Phys. Lett.*, vol. 95, p. 123119, 2009.

[17] R. Mohanty, A. Mishra, and J. Khatei, "Two-dimensional nanostructures for advanced applications: Adapting 2D nanomaterials for advanced applications," in *ACS Symposium Series*, American Chemical Society, 2020. doi: 10.1021/bk-2020-1350.

[18] S. M. Filipov, I. D. Gospodinov, and I. Faragó, "Replacing the finite difference methods for nonlinear two-point boundary value problems by successive application of the linear shooting method," *J. Comput. Appl. Math.*, vol. 358, pp. 46–60, 2019, doi: 10.1016/j.cam.2019.03.001.

[19] V. G. Palomar, "Metal film growth on weakly-interacting substrates: Multiscale modeling," Linköping University, Dept. Phys., Chem. Biol., 2020. doi: 10.3384/diss.diva-171435.

***Rehab N. Hasnawi (Corresponding Author)**
University of Basrah, Iraq
Email: rehab.naeem@uobasrah.edu.iq

Fatima H. Saeed
University of Basrah, Iraq